Dual-Polarized Probe with Full Octave Bandwidth and Minimum Scattering for Planar Near Field Measurements

A. Giacomini, V. Schirosi, R. Morbidini,
L. J. Foged

Microwave Vision Italy s.r.l.
Via dei Castelli Romani 59, Pomezia (Rome), Italy
{andrea.giacomini, lars.foged}@microwavevision.com

J. Estrada, J. Acree

MVG Inc.
2105 Barrett Park Dr., Suite 104
Kennesaw, Georgia 30144
United States of America
{john.estrada, jim.acree}@mvg-us.com

L. M. Tancioni
Orbit/FR Europe GmbH
Hans Pinsel Str. 7a
85540 Haar, Germany
lucat@orbitfr.de

Abstract — **Dual-polarized probes with wide-bandwidth operational capabilities are highly desirable for time-efficient Planar Near-Field (PNF) measurements [1]-[3]. However, sometimes the performance tradeoffs necessary to achieve the desired operating bandwidth make such probes impractical for many applications. Traditional probes are often bandwidth limited, and their electrical size can be an undesired source of scattering in PNF measurements, in particular if the probe-AUT distance is small [4]-[5]. An innovative, octave-band probe has recently been presented combining wide bandwidth, near constant directivity, low cross-polarization, and minimum scattering [6].**

In this paper, the probe design is discussed in detail, including technical and implementation trade-offs. Several probes have been manufactured at L/Ku-band band, and test results are presented. The probe design is fully scalable, even beyond Ka-band. The scattering properties of the probe (in terms of measurement perturbation) are assessed by numerical simulation and compared to standard rectangular open-ended waveguides.

I. INTRODUCTION

Traditional probes for Planar Near-Field (PNF) measurements are often Open-Ended Waveguides (OEW) with rectangular cross-section, known for their minimum physical dimensions [7] and polarization purity. Such probes offer half-octave bandwidth in single polarization. As an alternative, a circular OEW is often selected for its dual-polarization capabilities [8]. However, each solution has limitations on usable bandwidth, and the added drawback of an electrically larger aperture. The electrical size of the aperture is a primary source of probe scattering performance, although several other factors contribute to the scattering characteristics. The innovative probe presented in [6] fills a missing gap by combining all desirable characteristics for a PNF probe. Its main characteristics are full octave bandwidth and minimum scattering in dual polarization. The simple design makes it scalable for low and high frequencies, even beyond Ka-band.

An electrically small and axially symmetric aperture of 0.4λ diameter at the lowest frequency is the main contributor to the scattering minimization of the probe. The down-sizing of the aperture is obtained by a fully metallic design without the use of dielectric materials, making the design well suited for high power applications. The aperture provides a near constant directivity in the full bandwidth and low cross-polarization. A balanced ortho-mode junction (OMJ) with external circuitry, in order to obtain high polarization purity, feeds the probe. Table I. shows a performance comparison of the commonly used OEW probes for PNF measurements vs. the proposed design.

Table I. PNF MEASUREMENT PROBES

Features	Rectangular OEW	Circular OEW	Desirable PNF probe
Size	$0.6\lambda_{max}$ x $0.3\lambda_{max}$	$0.8\lambda_{max}$ diameter	$0.4\lambda_{max}$ diameter
Polarization	Single	Dual	Dual
Bandwidth	Half-octave	Half-octave	Full-octave or more
Reference	[7]	[8]	[6]
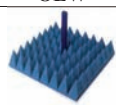
The organization of this paper is as follows: Section II introduces the main performance specifications; Section III deals with the probe design and trade-off considerations; Section IV illustrates the measured data across the entire bandwidth (0.8-20GHz); Section V presents an assessment of the scattering properties of the probe design to evaluate its contribution to the overall measurement uncertainty.

II. Performance Specifications

In addition to wide-band performance and dual-polarization capabilities, which are attractive features for time-efficient testing, PNF antenna measurements put additional requirements on the characteristics of the measurement probe [9]-[11]. Most of these specifications depend on the geometrical layout of the facility, i.e. the test distance and AUT size, but qualitative features beneficial for measurement accuracy can still be identified. These are summarized in Table II. The probe volumetric pattern in its forward hemi-sphere plays an important role in the illumination of the AUT. It should have sufficient dynamic range across the overall solid angle subtended by the AUT to effectively collect information from the AUT, without filtering or blinding any of its portions. Scattering properties of the probe are also relevant since they contribute directly to the probe-AUT interaction. This is known to be the main contributor to measurement accuracy in PNF measurements with short test distance [12].

Table II. Performance Specifications

Item	Specification	Comments
Polarization	Dual	H/V preferable
Bandwidth	/	trade-off with performance
Return loss	> 10dB	/
Isolation	> 45dB	for simultaneous acquisition (as independent RF channels)
Directivity	< 10dBi	in case of short probe-AUT distance, wide angle coverage, stable over frequency
Cross-polarization discrimination	> 45dB	on-axis, often additional value specified at probe field-of-view
Pattern shape	/	no side-lobes, no nulls in the forward hemisphere, equalised E/H cuts
Scattering	to be minimised	critical for measurement accuracy

III. Probe Design

The probe design presented in this paper is based on a wideband inverted quadridge OMJ, with balanced feeding enforced by external 3dB/180° hybrid couplers [13]-[15]. The inverted quadridge waveguide cross-section has been designed in order to achieve an electrically small cross-section while maintaining reasonable impedance values. The achieved inner diameter of the OMJ is on the order of approx. 0.4λ at the lowest operational frequency, representing roughly a 50% down-sizing compared to traditional hollow circular waveguides. The size reduction is obtained with a fully metallic design, without the use of dielectric materials and their physical shrinking effects, making this solution well-suited even for high-power applications. The OMJ feeds directly into an axially-symmetric tapered aperture of compact size. To avoid its cut-off, the inner conductor of the of the inverted quadridge waveguide is smoothly profiled, and protrudes from the aperture plane to avoid abrupt impedance discontinuities. The overall cross-section of the aperture is therefore minimized, and ensures low back-scattering properties. To further control the radiation pattern symmetry, increase the boresight directivity at the lowest frequencies, and minimize the front-to-back ratio, a recessed axial corrugation has been added externally.

Figure 1. shows a block diagram describing the OMJ and a cross-section of the probe radiating aperture with its recessed choke ring.
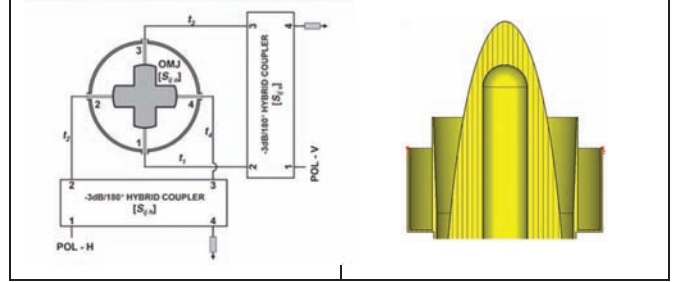
Figure 1. OMJ-based balanced inverted quadridge design (left), and detail of the probe radiating aperture (right).

At design stage, a trade-off has been carried out between maximum achievable bandwidth and acceptable performance in terms of the requirements presented in Section II. It was found that the main design parameters in conflict are the probe impedance versus the directivity levels and pattern shape. A bandwidth ratio between stop and start frequency of approximately 2.25 was found as achievable. This limit was further extended to 2.5 in the latest developments, but these developments are not covered in this paper. Following the outcome of this trade-off, the operational band ranging from L- to Ku-band (0.8-20GHz) was covered with six probes, including an overlap between the adjacent nominal bands of at least 15%. This overlap between probes was suggested by the measurement application, giving more flexibility and redundancy in use of the probes. A possible extension to Ka-band (40GHz) was also evaluated and, thanks to the design ease of scalability, this was considered realistic in terms of manufacturing constraints, even if not designed in practice as of this paper.

The probe design, referenced as DLP-PNF series, is depicted in Figure 2. for the L- and C-band versions, as taken from the mechanical CAD design. This figure shows the different parts of the probe assembly: the radiating aperture with recessed axial choke, the OMJ, the absorber screen, the stand-off housing, the precision feeding circuits, and the precision mounting interface at the probe bottom.
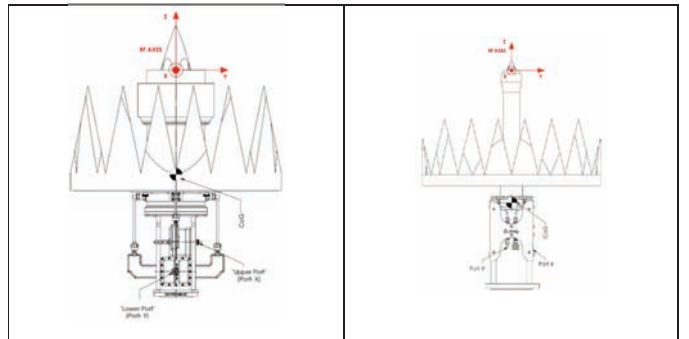
Figure 2. DLP-PNF-080 (left) and DLP-PNF-400 (right).

IV. MEASUREMENT DATA

After manufacturing, the DLP-PNF probes have been tested for input S-parameters and radiation pattern performance.

S-parameters referenced to 50Ohms have been measured in an anechoic environment for the six probes, and the results are shown in Figure 3. on the same graph. For briefness, only the return loss of X-port is presented, but the Y-port is nearly equivalent.
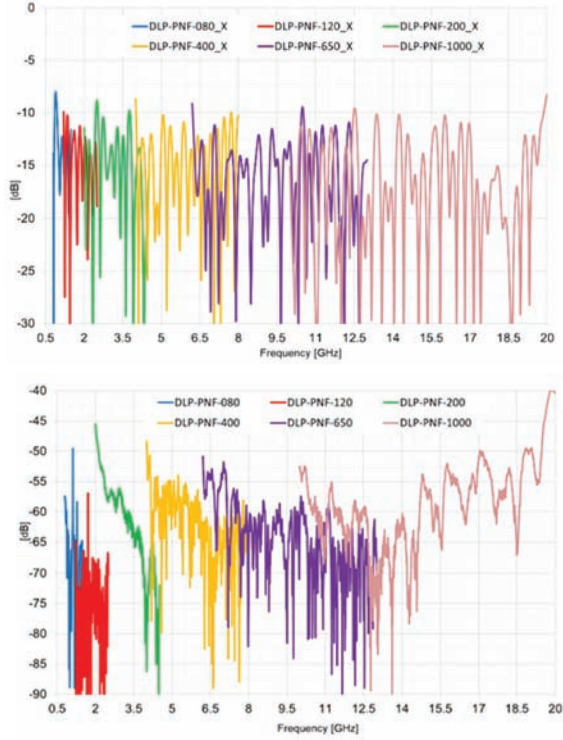
Figure 3.   Measured return loss of X port (top) and port-to-port coupling (bottom) referenced to 50 Ohms.

The oscillatory behaviour of return loss is typical of wideband antennas and due to constructive/destructive interference of the radiating aperture with the input ports. While undesirable, it is a trade-off that is tolerated to achieve wideband performance and can be fully compensated with probe correction. The worst case value exceeds the -10dB return loss only on a very few frequency points for each probe. Port-to-port coupling is also presented in Figure 3. Excellent performance is obtained with values significantly below 45dB, showing an excellent manufacturing accuracy and electrical symmetry of the feeding circuitry [16]. Only for the highest frequency band probe does performance show degradation, due to the use of the commercial hybrid couplers out of their nominal band (i.e 18-20GHz).

Verification testing was then extended to radiation pattern characteristics. The DLP-PNF models below 6GHz (080, 120, 200) have been measured for 3D gain-calibrated volumetric patterns in the SG64 [17] at MVG, Inc. (Atlanta, GA), while the higher frequency models (400, 650, 1000) have been tested in the StarLab 18GHz [18] at MVG Italy (Pomezia, IT).

Figure 4. and Figure 5. show the DLP-PNF under test in SG64 and StarLab 18GHz.
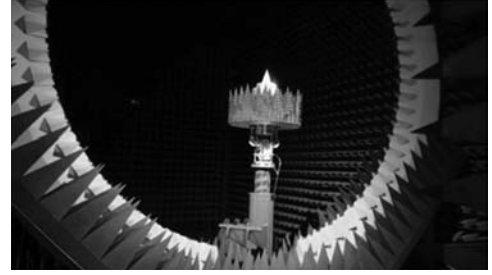
Figure 4.   DLP-PNF-080 under test in SG64, Atlanta (GA).
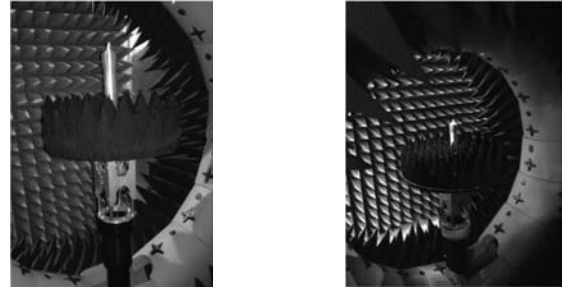
Figure 5.   DLP-PNF-400 and 650 under test in StarLab 18GHz, Pomezia (IT).

Table III.   presents a comprehensive summary of the relevant probe performances based on measured data. For the DLP-PNF-400, computed data was considered since the probe envelope exceeded the limits of the StarLab 18GHz in AUT maximum dimensions. Among the presented performances, it is noticeable that directivity remains sufficiently flat and well below the requirement (<10dBi) across the nominal bands. These directivity levels correspond to broad patterns of the probe, as demonstrated by the HPBW and the pattern dynamic range. This indicator is defined as the difference between the boresight directivity and minimum directivity within the +/-70° conical angle. Symmetry between E- and H-plane is also visible, with good cross-polarization performance including in the inter-cardinal planes, typical of corrugated circular apertures.

Table III.   SUMMARY OF DLP-PNF MEASURED PERFORMANCE

DLP-PNF	F start [GHz]	F stop [GHz]	BW	S11 [dB][2]	S21 [dB][2]	Directivity [dBi]
080	0.80	1.60	2.00	-7.3	-49.5	8.0 ± 1.0
120	1.20	2.50	2.08	-10.0	-56.9	8.4 ± 0.5
200	2.00	4.50	2.25	-8.8	-45.5	8.7 ± 0.8
400[1]	4.00	8.00	2.00	-8.7	-48.3	8.5 ± 0.3
650	6.20	13.00	2.10	-8.4	-50.8	8.1 ± 0.4
1000	10.00	20.00	2.00	-8.2	-39.2	8.2 ± 0.6

DLP-PNF	+/-70° pattern dynamic range [dB]	Min F2B [dB][3]	XPD +/-30° [dB][4]	HPBW 2x E-plane [deg]	HPBW 2x H-plane [deg]
080	11.9	15.0	20.1	88-53	92-63
120	12.4	15.0	22.4	78-53	87-67
200	14.0	16.1	19.7	74-48	84-62
400[1]	13.1	18.8	21.3	75-63	83-75
650	13.4	25.6	27.5	79-64	85-64
1000	15.3	30.6	17.7	77-58	87-64

1: All data of DLP-PNF-400 are simulated except S11 and S21 are measured
2: 50Ohms reference impedance, worst case value
3: F2B ratio is measured considering a pyramidal absorber panel with metal backing
4: Cross-polarization discrimination w.r.t. peak for |theta|<30°, all phi cuts

In addition to the performance indicators above, measured directivity pattern cuts have been compared with high-fidelity modeling [19]. The absorbing provisions have been included in the modeling in the configuration as-built. As commonly known, dielectric characteristics of absorbing materials are known with limited accuracy, and some deviations in the comparison may derive from this uncertainty. Figure 6. shows the correlation for the DLP-PNF-080 at the start frequency. Co-pol cuts correlate very well up to theta=90°, while some deviation is visible on the cross-pol levels. Figure 7. shows the same comparison for DLP-PNF-200 at an intermediate frequency, with general good agreement.
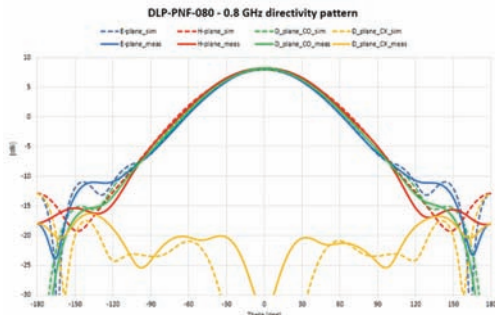
Figure 6.   Directivity pattern cuts @ 0.8 (start frequency) including absorbers.
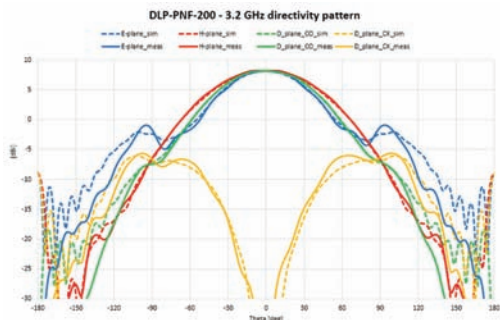
Figure 7.   Directivity pattern cuts @ 3.2GHz (intermediate frequency) including absorbers.

V. SCATTERING ASSESSMENT

In order to evaluate the scattering properties of the DLP-PNF design mentioned in Table II. , an EM assessment has been conducted by full wave simulations [19]. A PNF measurement scenario with a short separation using a Standard Gain Horn SGH1000 [20] as the reference AUT has been considered. This SGH is vertically-polarized, and operating at X-band (10-15GHz) with a boresight directivity of 25dBi at the center frequency. The simulated scenario shown in Figure 8. considers, for complexity reason only, the on-axis AUT-probe interaction, which is known to be the worst-case condition in terms of multiple reflections.
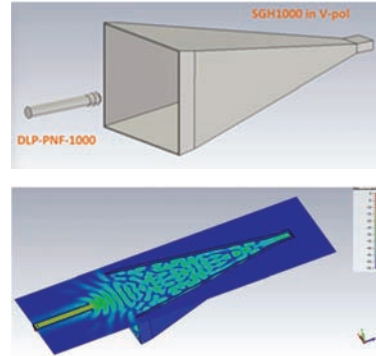
Figure 8.   EM scenario considered for scattering properties evaluation with an SGH as AUT.

This assessment has been carried out with the principle of comparing the actual DLP-PNF design with an Open-Ended Waveguide (OEW). These OEWs are well-known industry standards for PNF measurement, due to their low scattering properties.

In more detail, the evaluation is carried out by comparing the simulated VSWR over frequency of the three test cases reported in Figure 9. Initially, the VSWR is simulated transmitting from the SGH in free space, i.e. in absence of any measurement probe in front of the aperture. Then, an Open-Ended Waveguide (OEW) is placed at 3λ (@ 12.5 GHz) in V- and H- polarizations. Finally, the OEW is replaced by the dual-polarized DLP-PNF under investigation at the same distance. For the two probes in question, the feeding section is modelled by an ideal matched load, avoiding its re-radiation. This means that only the structural scattering properties of the probe apertures are compared in this exercise.
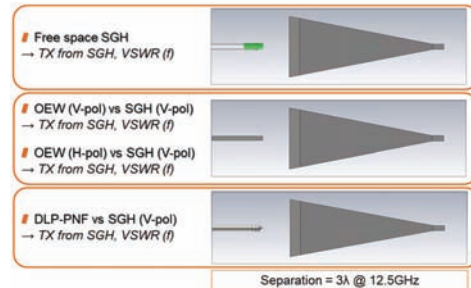
Figure 9.   EM scenario considered for scattering properties evaluation, with an SGH as AUT.

The collected VSWR curves over frequency are reported in Figure 10. By calculating the ratio between these VSWR curves and the free-space response, the interferer level induced by the probe presence is computed and presented in Figure 11.
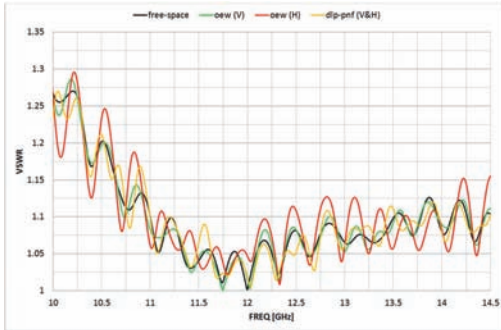
Figure 10. VSWR over frequency.

Probe	Interferer Level
OEW (V)	-34.0 dB
OEW (H)	-23.9 dB
DLP-PNF (V&H)	-29.4 dB

Figure 11. Interferer level induced by the probe presence in a PNF measurment: DLP-PNF versus OEW.

The interferer level induced by the OEW co-polarized with the AUT is -34.0dB and is the lowest interaction achievable in this scenario. When the OEW is rotated by 90° across its axis to collect the AUT cross-polarized field, the interferer becomes roughly 10dB higher. On the contrary, the DLP-PNF probe shows an interferer level of -29.4dB for both polarizations.

This finding is very interesting since, although the co-pol scattering of the OEW is less than the DLP-PNF probe, the cross-pol scattering of the OEW is severely worse, making the DLP-PNF probe particularly suited for demanding near-field measurements where both polarization components need accurate characterization.

VI. CONCLUSION

A Planar Near-Field probe design with full octave bandwidth capabilities has been presented. Its performance characteristics have been evaluated in this paper, discussing design considerations, trade-offs and experimental results. The probe technology has demonstrated excellent performance for testing scenarios in which the probe-AUT distance is short, and interaction is consequently a limiting factor in the overall measurement accuracy. The probe design has been manufactured and tested from L- up to Ku-band (0.8-20GHz), although the technology appears well-suited to cover the full frequency spectrum up to Ka-band (40GHz) due to its compactness, flexibility, and ease of scalability. In the near future, the assessment of the probe scattering properties will be further investigated through experimental activities, with a dedicated PNF measurement campaign.

REFERENCES

[1] ANSI/IEEE Std 149-1979 "IEEE Standard Test Procedures for Antennas";

[2] L. J. Foged, A. Giacomini, H. Garcia, S. Navasackd, C. Bouvin, L. Duchesne, "Wide-band dual polarized probe for accurate and time efficient satellite EIRP/IPFD measurements" AMTA 2005, Oct. 30-Nov. 4, Newport, RI;

[3] L.J. Foged, A. Giacomini, R. Morbidini, "Dual-Polarized corrugated horns for advanced measurement applications", Antennas & Propagation Magazine, Vol 52, No 6, December 2010;

[4] C.G.M. van 't Klooster, "On probes for planar near-field measurements", 33rd ESA Antenna Workshop on Challenges for Space Antenna Systems, 18-21 October 2011, ESA/ESTEC, Noordwijk, The Netherlands;

[5] J. Bach Andersen, A. Frandsen, "Absorption Efficiency of Receiving Antennas", IEEE Transactions on Antennas and Propagation, vol. 53, no. 9, September 2005;

[6] A. Giacomini, L. J. Foged, R. Morbidini, L.Tancioni, J. Estrada, J. Acree "Minimum Scattering Probe for High Accuracy Planar NF Measurements", AMTA 2016, Oct. 30 – Nov. 4, Austin, TX;

[7] http://www.mvg-world.com/en/system/files/datasheet_antenna_2016_hd_open_ended_waveguides.pdf

[8] http://www.mvg-world.com/en/products/field_product_family/antenna-1/dual-polarized-open-ended-waveguide-interchangeable

[9] L. J. Foged, A. Giacomini, "Wide-Band Dual Polarized Probes for Near Field Antenna Measurements", IEEE International Symposium on Antennas and Propagation 2007, June 10-15, Honolulu, HI;

[10] L. J. Foged, A. Giacomini, R. Morbidini, N. Isman, "Wideband Dual Polarized Probe with Interchangeable Apertures for Advanced Antenna Measurement Applications", APS/URSI Symposium July 11-17, 2010 Toronto, Ontario, Canada;

[11] L. J. Foged, A. Giacomini, R. Morbidini, "Dual Polarized Probe for Wideband Planar Near Field Measurement Applications", 5th European Conference on Antennas and Propagation, EuCAP 2011, Rome, Italy, 11-15 April 2011;

[12] A. C. Newell, "Error Analysis Techniques for Planar Near-Field Measurements", IEEE Transactions on Antennas and Propagation, Vol. 36, No. 6, June 1988;

[13] SATIMO Patent, 2010-02-11, Inventors: Foged Lars Jacob, Giacomini Andrea, Duchesne Luc, Publication number: US2010033264 (A1), FR2907601 (A1), WO2008049776 (A1), EP2092592 (A1), "Orthogonal-mode junction coupler with an ultra-broad operating bandwidth";

[14] L. J. Foged, L. Duchesne, L.Roux, Ph. Garreau, "Wide-band dual polarized probes for high precision near-field measurements", AMTA 2002, 3-8 Nov, Cleveland, OH;

[15] L. J. Foged, A. Giacomini, L. Duchesne, C. Feat, "Wide-band dual polarized probes for near field antenna measurements" AMTA 2006, October 22-27, Austin, TX;

[16] L. J. Foged, A. Giacomini, R. Morbidini, "Probe performance limitation due to excitation errors in external beam forming network", AMTA 2011, October 16-21, Englewood, CO;

[17] http://www.mvg-world.com/en/system/files/SG64_2014_bd.pdf

[18] http://www.mvg-world.com/en/system/files/starlab_2014.pdf

[19] www.cst.com, CST STUDIO SUITE™, CST AG, Germany;

[20] http://www.mvg-world.com/en/system/files/datasheet_antenna_2016_hd_standard_gain_horns.pdf